Tilted fibre Bragg grating based 800nm WDM interrogation system for strain, temperature and refractive index sensing

Rui Suo*[a], Xianfeng Chen[a], Kaiming Zhou[a], Lin Zhang[a], Ian Bennion, Bo Liu[b]
[a]Photonics Research Group, Aston University, Birmingham, UK, B47ET;
[b]Institute of Modern Optics, Nankai University, Tianjin, P.R.China, 300071

ABSTRACT

We report the implementation of a low-cost high-resolution WDM interrogation system operating around 800nm region with bandwidth up to 60 nm and resolution of 13 pm by utilising a tilted fibre Bragg grating as an out-coupling device and a CCD-array detector. The system has been evaluated for interrogating fibre Bragg grating based strain, temperature sensors, giving sensitivities of 0.6 pm/με and 5.6 pm/°C which are in good agreement with previously reported values. Furthermore, the system has been utilised to detect refractive index change of sample liquids, demonstrating a capability of measuring index change as small as 10^{-5}.

Keywords: Tilted fibre Bragg grating, WDM interrogation system, Optical sensing

1. INTRODUCTION

Tilted fibre Bragg gratings (TFBGs) were previously shown to have the ability to couple the light out of the fibre core and thereby being implemented as optical taps[1]. Side detection interrogation techniques employing a TFBG and photo-detectors were also reported[2,3]. Quite recently, by utilising the out-coupling function of a TFBG, Simpson *et al* have demonstrated an in-fibre WDM spectrum analyser with an operation range around 1550nm[3]. In this paper, we report an implementation of a WDM interrogation system operating around 800nm range using a TFBG and a low-cost CCD-array detector. The system has been evaluated for strain, temperature and refractive index sensing with performance close to other techniques. However, the merit of low-cost, high-resolution and compact size could make this system much more attractive for industrial applications.

A TFBG is capable of coupling light out of the fiber core in diverse directions with different strengths. If the tilted angle is < 45°, the light will be coupled to the backward-propagating cladding and radiation modes. The strongest light coupling occurs at the wavelength determined by the phase match condition:

$$\lambda_{co-cl} = \left(n_{co} + n_{cl,m}\right) \cdot \frac{\Lambda}{\cos\theta} \tag{1}$$

where n_{co} and $n_{cl,m}$ are the effective mode indexes of fundamental core and mth cladding modes, respectively, Λ is the grating period and θ is the tilt angle of the structure.

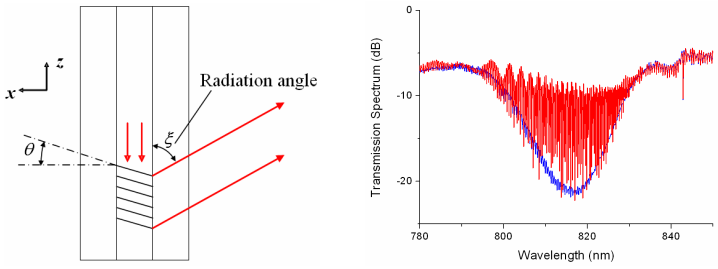

(a) (b)

Fig.1 (a) TFBG geometrics showing the tilt (θ) and radiation (ξ) angles. (b) Transmission spectrum of a $7°_{ext}$-TFBG in 800nm range.

*suor@aston.ac.uk; phone 0044 121 204-3548; fax 0044 121 204-3682

Third European Workshop on Optical Fibre Sensors, Antonello Cutolo, Brian Culshaw, José Miguel López-Higuera, Eds.,
Proceedings of SPIE Vol. 6619, 66192N, (2007) · 0277-786X/07/$18 · doi: 10.1117/12.738679

By further deduction from phase-match condition[4], the radiation angle (ξ) of the coupled light of certain wavelength (λ) in the radiation range of TFBG is related to the period (Λ) and tilt angle (θ) as follows:

$$\tan(\xi) = \frac{\lambda \sin(\theta)}{\lambda \cos(\theta) - n\Lambda} \tag{2}$$

where n represents the refractive index of the fibre (ignoring the difference between core and cladding).

2. 800NM WDM INTERROGATION SYSTEM

2.1 System setup

The WDM interrogation system is shown schematically in Fig 2(a). A 7°$_{ext}$-TFBG UV-written in hydrogenated 820nm single mode fibre was employed as the out-coupling device in this system. The TFBG was mounted on a rotational stage to enable the direction of the radiated light to be controlled, and immersed in index matching gel to transfer the coupled light from cladding to radiation modes. A cylindrical lens was used to collimate the radiation light from the TFBG to the CCD-array. The Sony ILX511 CCD-array consisting of 2048 14μm-pixels was mounted on a motorised translation stage to be moveable along y-axis direction for scanning the radiation profile. A contour plot obtained by scanning the CCD-array is shown in Fig.2 (b).

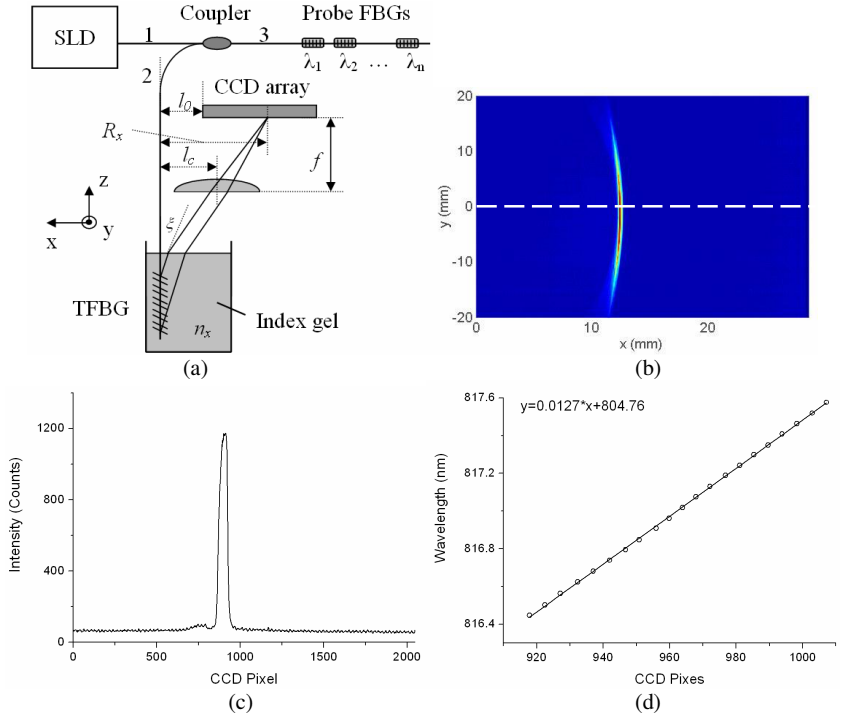

Fig.2 (a) Schematic diagram of the apparatus used for the TFBG-CCD interrogation system. (b) Contour plots in x-y plane showing the far-field image of radiated light captured by the CCD-array. (c) An example of intensity signal captured by the CCD. (d) Calibration plot of wavelength changing against CCD pixel shift.

2.2 Spectrum analyser function

The illumination profile shifts along the CCD-array in x-direction with the wavelength change of the TFBG input. Therefore, the wavelength can be decoded from the illumination position on the CCD. The correlation between the wavelength of the input signal and the pixel position on CCD was calibrated by performing a strain sensing experiment on an FBG with 816.45nm Bragg resonance, and plotted in Fig.2 (d), giving a conversion coefficient of 12.7pm/pixel.

The bandwidth of the system is limited by the detection-length of CCD-array, the focal length of lens and the radiation mode spectrum of TFBG. With a 7°$_{ext}$-TFBG and the given CCD, we calculated the system parameters (bandwidth, conversion coefficients) for two focal lengths, as shown in Table 1.

Table 1. System parameters for two different focal lengths

Focal length (mm)	Bandwidth (nm)	Gradient (nm/mm)	Physical resolution (pm/pixel)
45	60	3.34	47
155	26	0.91	13

Considering using the most detection length of the CCD-array, a cylindrical lens with a 155mm focal length was employed in the system to perform strain and temperature sensing experiment using the FBG mentioned above. The strain changes from 0$\mu\varepsilon$ to 2000$\mu\varepsilon$ with an incremental step of 100με and the temperature variations from 0˚C to 60˚C in a step of 2˚C were applied to the FBG respectively. The measured strain and temperature responses of the FBG are plotted in Fig.3 (a) and (b), respectively. The strain and temperature sensitivities are estimated from the plots as 0.6 pm/με and 5.6 pm/˚C, which are in good agreement with previously reported typical results of 0.64 pm/με and 6.8 pm/˚C around 830nm[5].

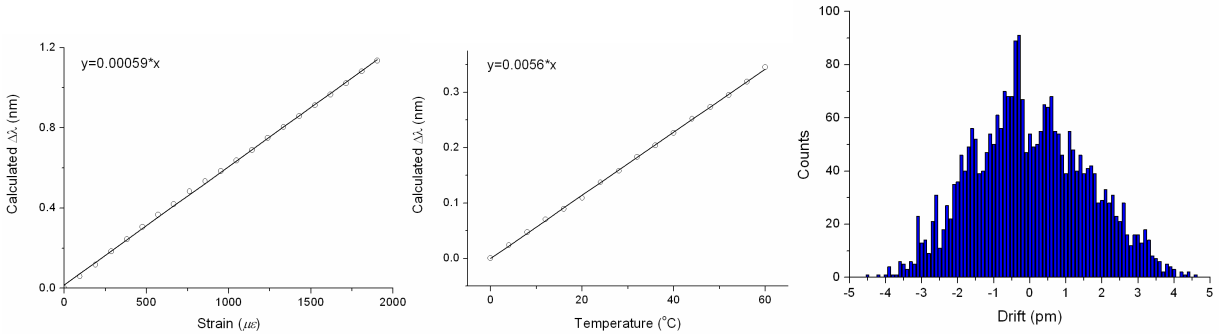

(a) (b) (c)

Fig.3 Spectral shift of sensing FBG against (a) strain and (b) temperature measured by the TFBG-CCD interrogation system. (c) Histogram to show the distribution of the recorded wavelength drifts over a 45-min period.

In order to ascertain the stability of the system, we stabilised the sensor FBG at 20˚C and monitored the output signal from the TFBG for 45 min with a sample rate of 1 Hz. The histogram is shown in Fig.3 (c) displaying the distribution of the recorded wavelength drifts that form a clear normal distribution. The root mean square (RMS) deviation from the mean of this histogram is a mere 1.6 pm, which indicates that the system is inherently stable.

2.3 Refractive index sensing

With a fixed probe light, the system can also be applied to measure the surrounding-medium refractive index (SRI) of the TFBG. Thus, this system has the capability for detecting bio/chemical samples, which may have a potential use for medicine, environmental monitoring and lifescience applications. As shown in Fig.2 (a), the distance from the fibre to the focal point R_x (named as radiation radius) is related to the refractive index of the liquid, n_x, as follows:

$$R_x = l_c + f \cdot \sqrt{\frac{n_x^2 - n^2\cos^2(\xi)}{1 - n_x^2 + n^2\cos^2(\xi)}} \tag{3}$$

where l_c represents the distance between the fibre and the centre of the lens and f is the focal length.

The system bandwidth for SRI measurement is also limited by the focal length and the detection dimension of CCD-array. Considering a common SRI range from 1.3712 to 1.4735, the radiation radius R_x can be calculated according to equation (3). Table 2 lists the calculated R_x values for two focal lengths (45mm and 155mm). For a given CCD position, we can derive the relationship between the CCD pixels and radiation radius as

$$N = (R_x - l_0)/0.014 \tag{4}$$

where, l_0 is the position of the first pixel point in the CCD-array and 0.014 is a single pixel size in mm. From table 2, we can see that giving l_0 = ~33mm and for SRI range 1.3712 to 1.4735, a lens of 45mm focal length is more suitable to use the most CCD-array detection area (~28mm).

Table 2. Calculated radiation radii with various sample liquid refractive indexes

n_x	1.3712	1.3848	1.3988	1.4132	1.4280	1.4432	1.4589	1.4735
R_x (f=45mm)	31.52	35.82	39.29	42.46	45.52	48.57	51.74	54.74
R_x (f=155mm)	49.90	64.72	76.66	87.58	98.13	108.70	119.56	129.89

The theoretical simulation of the radiation radius R_x against the refractive index of sample liquid n_x is plotted in Fig.4 (a). It can be seen from the figure that the entire correlation between R_x and n_x is non-linear, but the range from 1.40 to 1.55 is nearly linear. In the experiment, five sample liquids with refractive indices distributed from 1.4132 to 1.4735 were selected for SRI sensing evaluation. Fig.4 (b) plots the correlation between SRI and CCD pixels, showing a near-linear response. Since a single pixel of CCD-array can be readily resolved, from the plot we can estimate that the SRI change as small as ~10^{-5} should be detectable by this system.

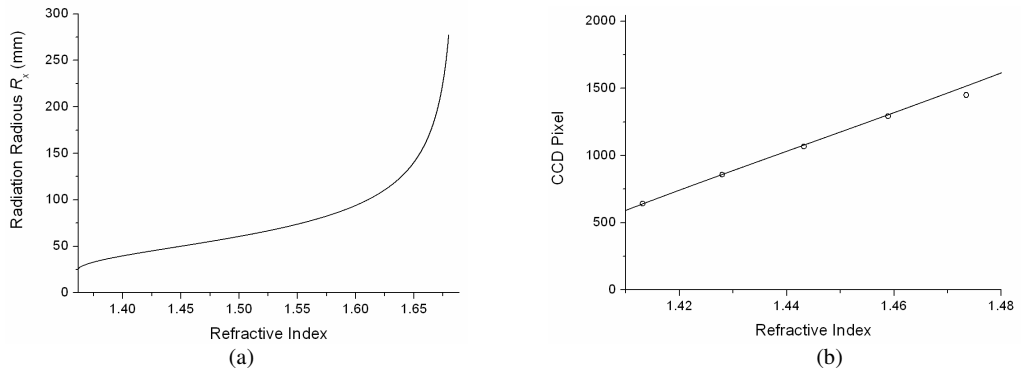

Fig.4 (a) The theoretical simulation plot of the radiation radius R_x against the refractive index of sample liquid n_x in the range from 1.36 to 1.68; (b) the CCD pixels against refractive index change of measured sample liquid: open circles are the measured values and the line is simulation results converted from radiation radius to pixels.

3. CONCLUSION

We have demonstrated a TFBG based 800nm WDM interrogation system, which can function as an in-fibre spectrum analyser with an interrogation bandwidth up to 60 nm and a resolution of 13 pm. The system was evaluated by performing the FBG strain and temperature sensing experiments, obtaining the strain and temperature sensitivities of 0.6 pm/με and 5.6 pm/°C, which are in good agreement with the reported typical values. In addition, the system was further evaluated for sensing the refractive index of sample liquid. In the near-linear range from 1.4132 to 1.4735, we estimate that the SRI change as small as ~10^{-5} can be detected by this low-cost high-resolution TFBG WDM interrogation system.

REFERENCE

1. G. Meltz, W. W. Morey, and W. Glenn, "In-fibre Bragg grating tap," *Optical Fibre Communications Conference*, Optical Society of America, Washington, D.C., 1990, TuG1.
2. J. L. Wagener, T. A. Strasser, J. R. Pedrazzani and J. Demarco, "Fiber grating optical spectrum analyzer tap," *ECOC 97*, 65-68 (1997).
3. A. G. Simpson, K. Zhou, L. Zhang, L. Everall, and I. Bennion, "Optical sensor interrogation with a blazed fiber Bragg grating and a charge-coupled device linear array," *Appl. Opt.*, 43 (1), 33-40 (2004).
4. K. Zhou, L. Zhang, X. Chen and I. Bennion , "Low thermal sensitivity grating devices based on ex-45° tilting structure capable of forward-propagating cladding modes coupling," *J. Lightwave Technol.,* 24 (12), 5087-5094 (2006).
5. Y. J. Rao, "In-fibre Bragg grating sensors," *Meas. Sci. Technol.*, 8, 355-375, (1997).